Proceedings of the VIII Mediterranean Conference
on Medical and Biological Engineering and Computing

14-17 June 1998
Lemesos, Cyprus

Non-stationary texture segmentation in electron microscopic muscle imaging

Marios S. Pattichis †, *Constantinos S. Pattichis* ‡, *Maria Avraam* ‡, *Alan C. Bovik* †, *Kyriakos Kyriakou* *

†Laboratory for Vision Systems, University of Texas, Austin, TX 78712-1084
e-mail: {marios, bovik}@vision.ece.utexas.edu

‡Department of Computer Science, University of Cyprus, Nicosia, Cyprus
e-mail: pattichi@turing.cs.ucy.ac.cy

*Department of Electron Microscopy, The Cyprus Institute of Neurology and Genetics, Nicosia, Cyprus
e-mail: Kyriacos@mdrtc.cing.ac.cy

Abstract

We segment electron microscope images using a novel AM-FM representation for separating out the structural units of the muscle. This novel AM-FM approach is shown to be both effective and accurate in capturing sarcomeres and mitochondrial regions of the electron microscope images.

1 Introduction

Accurate diagnosis of some neuromuscular disorders requires examination of muscle biopsies with the electron microscope. Ultrastructural examination is often essential for confirming the diagnosis of metabolic myopathies and in particular those myopathies that are caused by mitochondrial abnormalities. Such abnormalities cause the accumulation of mitochondrial aggregates which disturb the very regular anatomic pattern exhibited by normal muscle fibres characterized by the repetitive arrangement of functional units, called sarcomere.

In some patients, suspected of suffering from mitochondrial abnormalities, the mitochondrial aggregates are not as pronounced, making diagnosis difficult. In order to overcome this difficulty a non-stationary texture segmentation method has been applied to electron microscopic muscle images. The main objective is to train the system on recognizing abnormalities that disturb the regular sarcomere structure of muscle fibres using known "typical" diagnostic cases. The ultimate objective will be to test the ability of the system to recognize "pathological abnormalities" in borderline cases in order to supplement the diagnostic ability of human experts.

2 Method

In Figures 1 (a) and 1 (b), we show the two examples of the electron microscope images that we studied. In the normal image, in Figure 1 (a), the repetitive arrangement of the sarcomeres is displayed. Before extracting the muscle tissues, the sarcomeres were perfectly aligned. After extracting the tissue, the alignment was broken, resulting into sharp boundaries between the different units. For the pathological tissue, the mitochondrial abnormalities are shown in Figure 1 (b). The abnormal regions are seen to overtake the sarcomeres, effectively destroying the regular structure of the normal muscle. We want to identify these abnormal regions.

The underlying characteristic for both Figures 1 (a) and 1 (b) is the repetition of the sarcomeres, and the repetition of the myofilaments within each unit. This observation suggests that the images should be analyzed at two spatial resolution levels: (i) a low spatial resolution level where the myofilaments are not resolved, but the sarcomeres are resolved, and (ii) a high spatial resolution level where both the myofilaments and the repeating sarcomeres are to be resolved. Naturally, we expect that the abnormal mitochondrial regions can be identified at both resolution levels. For the purposes of this paper, we focus our attention to the low spatial resolution level, leaving the high resolution level for a later study.

At both resolution levels, we are interested in high quality results, where spatial resolution cannot be sacrificed, yet the structure of the images is dominated by repeating patterns. To describe the repeating patterns, a spatial-frequency model was used. Unfortunately, wavelet models cannot be used without sacrificing precious spatial resolution because wavelet transforms employ downsampling, losing half of our spatial resolution for each downsampling operation performed. This is not the case for AM-FM transforms [3] (see earlier work in [1]). In AM-FM representations, the instantaneous frequency and amplitude are defined at every point in the image and hence there are no limits in spatial resolution.

Next, we introduce two distinct AM-FM series expansions for describing mitochondrial regions and sarcomeres. For sarcomeres, constant intensity level curves run across the units; we can trace a sacromere from (for example) the left boundary of the unit to the right boundary. For the mitochondrial regions, this is clearly not the case. The mitochondrial regions are made of a collection of dark circles on a white regions. Clearly, the boundary of any particular circle does not connect the boundary of the entire mitochondrial region.

This elementary observation helps guide us in selecting the appropriate AM-FM series expansion (see [3] for a list of many possible AM-FM series expansions). For the sarcomeres, we use a sequence of FM harmonics $\exp j\phi(\mathbf{x})$, $\exp j2\phi(\mathbf{x})$, ... that all share the same level curves of constant intensity: $\exp jn\phi(\cdot)$ is constant along any curve along which $\phi(\cdot)$ is constant. To account for slow variations from this model, we use a slowly varying amplitude $a(\cdot) > 0$ defined to be non-zero only throughout the extends of the sarcomere:

$$a(\mathbf{x}) > 0, \quad \text{for } \mathbf{x} \in S_i, \qquad a(\mathbf{x}) = 0, \quad \text{for } \mathbf{x} \notin S_i$$

where S_i is the set of pixels where the sarcomere is defined. Thus, for each sarcomere, we write

$$I_i(\mathbf{x}) = \sum_n G_{i,\,n} a_i(\mathbf{x}) \exp\Big[\; jn\phi(\mathbf{x}) \;\Big]$$

and for the collection of all sarcomere units, we have

$$I_s(\mathbf{x}) = \sum_n G_{1,\,n} a_1(\mathbf{x}) \exp\Big[\; jn\phi_1(\mathbf{x}) \;\Big] + \sum_n G_{2,\,n} a_2(\mathbf{x}) \exp\Big[\; jn\phi_2(\mathbf{x}) \;\Big] + \cdots + \sum_n G_{M,\,n} a_M(\mathbf{x}) \exp\Big[\; jn\phi_M(\mathbf{x}) \;\Big]$$

For the mitochondrial regions, the required AM-FM series is a generalization of the 2-d Fourier series where we allow for intensity variations along a curvilinear coordinate system [3]:

$$I_m(\mathbf{x}) = \sum_{n,\,m} F_{1,\,n,\,m} a_{M+1}(\mathbf{x}) \cos\Big[\; n\psi_{1,\,1}(\mathbf{x}) + m\psi_{1,\,2}(\mathbf{x}) \;\Big] + \cdots + \sum_{n,\,m} F_{Q,\,n,\,m} \cos\Big[\; n\psi_{Q,\,1}(\mathbf{x}) + m\psi_{Q,\,2}(\mathbf{x}) \;\Big]$$

and for the entire image, we have the sum of the two expansions $I(\mathbf{x}) = I_s(\mathbf{x}) + I_m(\mathbf{x})$.

The fundamental question to address next is how many AM-FM harmonics should we use: what is M and Q? In the absence of mitochondrial regions, when lines of constant intensity run across the image (with possible breaks over sets of measure zero (zero area)), we then group all local expansions into one ($M = 1$). When mitochodrial regions do exist, then we can still groups local AM-FM expansions for as long as the resulting AM-FM expansions are defined over connected sets. Hence, the minimum number of M is simply the minimum number of connected sets that cover the sarcomere regions. Similarly, for mitochondrial regions, the minimum number of Q corresponds to the minimum number of connected sets that cover the mitochondrial regions.

For seperating out the different image segments, we use the fundamental AM-FM components from each sarcomere region

$$G_{1,\,1} a_1(\mathbf{x}) \exp\Big[\; j\phi_1(\mathbf{x}) \;\Big],\; G_{2,\,1} a_2(\mathbf{x}) \exp\Big[\; j\phi_2(\mathbf{x}) \;\Big],\; \ldots,\; G_{M,\,1} a_M(\mathbf{x}) \exp\Big[\; j\phi_M(\mathbf{x}) \;\Big]$$

and from each mitochondrial region

$$F_{1,1,0}a_{M+1}(\mathbf{x})\exp\Big[\ j\psi_{1,1}(\mathbf{x})\ \Big],\ \ldots,\ F_{Q,1,0}a_{M+Q}(\mathbf{x})\exp\Big[\ j\psi_{Q,1}(\mathbf{x})\ \Big].$$

For the mitochondrial regions, we recognize that we had two possibilities for the fundamental AM-FM haromonic, either $F_{i,1,0}a_{M+i}(\mathbf{x})\exp\Big[\ \psi_{i,1}(\mathbf{x})\ \Big]$ or $F_{i,0,1}a_{M+1}(\mathbf{x})\exp\Big[\ \psi_{i,2}(\mathbf{x})\ \Big]$. For simplicity, and without loss of generality, we relabel the two harmonics so that the one corresponding to $\psi_{1,1}(\cdot)$ captures more energy $|F_{i,1,0}| \geq |F_{i,0,1}|$. We leave the details on how to compute these fundamental AM-FM components for Section 3.

Once the fundamental AM-FM components have been determined, we use the local amplitude $a(\cdot)$ and/or the local instantaneous frequency magnitude ($\| \nabla\phi_i(\cdot) \|$ or $\| \nabla\psi_{i,1}(\cdot) \|$), to isolate the mitochondrial regions from the sarcomere regions. We expect the range of values for these two AM-FM parameters to be different for the sarcomere and the mitochondrial regions. This observation will be the basis of our segmentation algorithm.

3 Implementation

In this Section, we discuss how to use the dominant component analysis algorithm to estimate the fundamental AM-FM components, and then apply simple thresholding to isolate the mitochondrial regions.

As we discussed, we must first isolate the fundamental AM-FM components. To this end, we prefilter the image using an ideal, circularly symmetric, lowpass filter with a circular radius cutoff at 0.15 cycles per image length. The cutoff frequency allows AM-FM harmonics with an instantaneous wavlength of about 7 pixels and was empirically determined to be sufficient. Next, to estimate the AM-FM harmonics, we use the dominant component analysis (see [2] for details). In the dominant component analysis algorithm, a bank of Gabor channels is applied to the image, and the channel with the maximum energy is selected for estimating the AM-FM parameters. If we let $t_m(\cdot)$ denote the channel output at the mth channel with frequency magnitude response $G_m(\cdot)$, then the AM-FM parameters are given by [2]:

$$\nabla\Phi(\mathbf{x}) \approx \mathrm{Re}\left[\frac{\nabla t_m(\mathbf{x})}{j t_m(\mathbf{x})}\right], \quad \Phi(\mathbf{x})\arctan\left\{\frac{\mathrm{Im}[t_m(\mathbf{x})]}{\mathrm{Re}[t_m(\mathbf{x})]}\right\}, \quad a(\mathbf{x}) \approx \left|\frac{t_m(\mathbf{x})}{G_m[\nabla\hat{\theta}\mathbf{x}]}\right|$$

For our purposes, we are only interested in the amplitude $a(\cdot)$ and the instantaneous frequency magnitude $\| \nabla\phi(\cdot) \|$. To isolate the structural units of the muscle, we select thresholds for $a(\cdot)$ and $\| \nabla\phi(\cdot) \|$ using the histogram of the distribution of their values (see Figures 1 (c)-(f)). For the instantaneous frequency magnitude, we threshold between the low peaks of the histogram, while for the amplitude, we threshold at a level that appears to be at the right end of the main distribution (see the caption in Figure 2 for details).

4 Results

We present the segmentation results in Figures 2 $(a)-(h)$. In order to analyze the resulting images, we first explain briefly how the values of the amplitude and the instantaneous frequency can be associated with the local structure variations of the electron micrographs. We then comment on the segmented images.

We first explain (briefly) what the AM-FM parameters are measuring. For the amplitude, we note that it describes the bounds in the local intensity variations. For example, when the local image intensity is alternating between nearly white (maximum intensity) and nearly black (minimum intensity) values, then the local amplitude is indeed large. On the other hand, when the local image intensity alternates between small variations of gray intensity, the amplitude is small. For the instantaneous frequency magnitude, we note that it is inversely proportional to the instantaneous wavelength, that is the period of the locally repeating pattern. When the repeating pattern is thin, the instantaneous wavelength is small and the instantaneous frequency magnitude is large. When the repeating pattern is thick, the instantaneous wavelength is large, and the instantaneous frequency magnitude is small. Since we are estimating the fundamental AM-FM components, we also expect that the segmented images will be made of regions that are as thick as the fundamental wavelength.

The sarcomeres are separated by sharp dark and white regions. Recalling our intutive characterization of the AM-FM parameters, we note that between any two sarcomeres, there is large variation above and below the "local mean" image intensity, and this is described by large fundamental amplitude components for the regions between the units:

$$|G_{i,\,1}a_i(\mathbf{x})| \gg |G_{j,\,1}a_j(\mathbf{x})|$$

when S_i corresponds to a boundary region, while S_j corresponds to a normal sarcomere region. Similar comments apply for the mitochondrial regions. The dark mitochondria on a white background yield very large amplitude components. This observation makes it difficult to differentiate between sarcomere boundaries and mitochondrial regions, if we only use the range of amplitude values for this purpose. Nevertheless, this observation suggests a method for differentiating mitochondria and sarcomere boundary regions from the main sarcomere units (see the results of Figures $2(a) - (b)$, where an amplitude level over 20 is considered to be high).

We now turn to the instantaneous frequency magnitude results $\| \nabla \phi_i(\cdot) \|$. Clearly, the white and dark stripes at the boundaries of the sarcomer units are thin as compared to the size of the sarcomer units. Thus, they are characterized by large instantaneous frequency magnitude $\| \nabla \phi_1(\cdot) \|$. This observation is clearly demonstrated in the resulting images in Figures $2(c), (e), (g)$, and also in $2(d), (f), (h)$.

Next, we comment on the segmented images. First, we comment on the results for the normal case. Overall, the boundaries of the sarcomeres have been successfully detected (see Figures 2 (a) and (e)). Furthermore, the mid-region of the sarcomeres which correspond to the I bands are also successfully detected as shown in Figure 2 (g). The rest of the sarcomers have also been detected (as shown in Figure 2 (c)). It is evident that in these images a regular repetitive pattern is displayed which closely approximates the normal fibre structure of physiological muscle fibres.

Next, we comment om the results for the case suspected as having mitochondrial abnormalities. A definite diagnosis of mitochondrial myopathy could not be made so this was considered as borderline case. The amplitude segmented image (of Figure 2 (b)) shows that the proposed system has the potential to identify the abnormal regions. Normal regions are also included in Figure 2 (b), indicating that the system should be further enhanced in order to enable it to cope with difficult cases such as the example presented. The instantaneous frequency magnitude results of Figures 2 (d), (f) and (h) were less impressive than the corresponding images for the normal case. Nevertheless, the amplitude results of Figure 2 (b) are very promising, and it can be seen that the instantaneous frequency magnitude results can be combined with the amplitude results to improve performance (as for example by removing the sarcomeres detected in Figures $2(f)$ and $2(h)$ from the mixed sarcomere-mitochondrial regions of Figure $2(b)$).

5 Concluding Remarks

Our findings although preliminary suggest that the proposed system has the potential to identify normal repetitive structure, with a good degree of accuracy. Furthermore the system is capable of detecting abnormal regions which disturb the regular pattern, such as those present in musle pathology. More work is currently being carried out in order to make the system recognition more sensitive and impose its specificity. The wider applicapility of such systems will also enhance our ability to quantify changes that affect the cellular ultrastructure.

References

[1] A. C. Bovik, N. Gopal, T. Emmoth, and A. Restrepo. Localized measurement of emergent image frequencies by Gabor wavelets. *IEEE Trans. on Information Theory*, 38(2):691–712, March 1992. Special Issue on Wavelet Transforms and Multiresolution Signal Analysis.

[2] J. P. Havlicek. *AM-FM Image Models.* PhD thesis, The University of Texas at Austin, 1996.

[3] M. S. Pattichis. *AM-FM Transforms with Applications.* PhD thesis, The University of Texas at Austin, 1998.

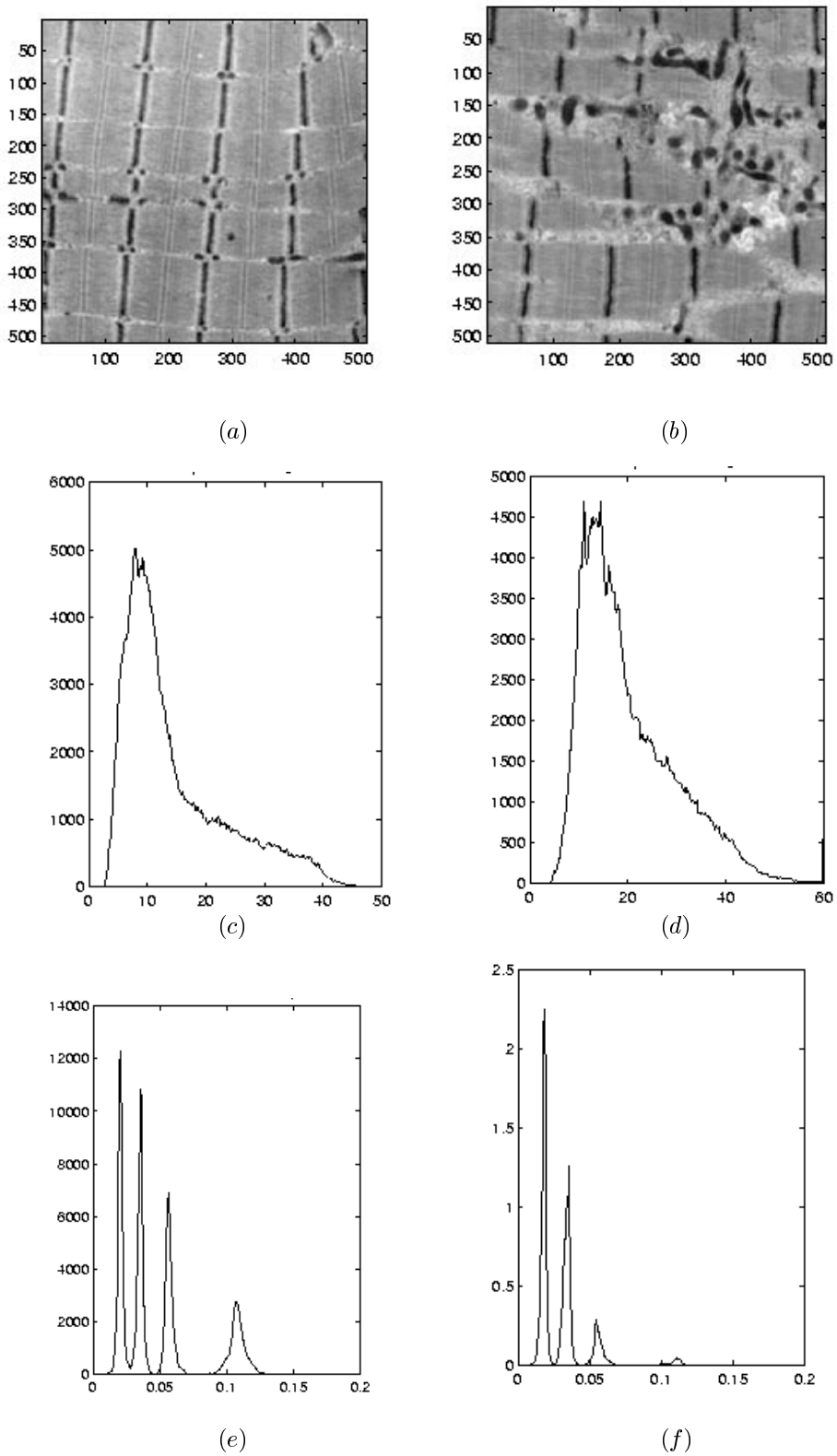

Figure 1: AM-FM analysis results I of II. In (a), we show a normal, electron microscopy image. In (b), we show a pathological case. In (c) and (d) we show the histograms of the amplitude $a(\cdot)$ distribution for all local AM-FM components. Similarly, in (e) and (f), we show the histograms of the instantaneous frequency magnitude (note that in (f) the frequencies must be multiplied by 1000 and the units are cycles per image length).

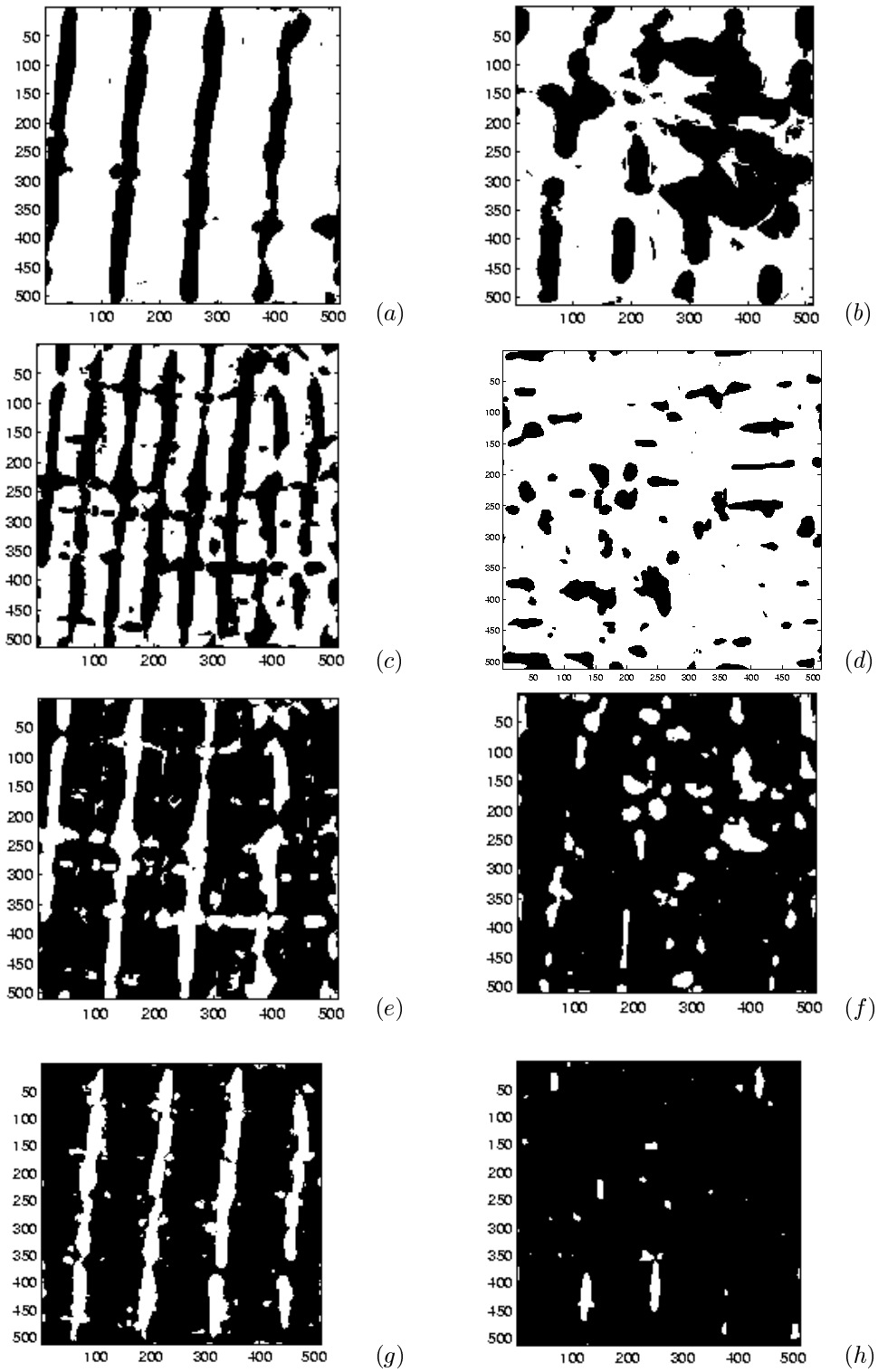

Figure 2: AM-FM analysis results II of II. In (a), (c), (e) and (g) we present results for the normal image, while in (b), (d), (f) and (h) we present results for the pathological image. For (a) and (b), we show the results for thresholding the amplitude: $a(\cdot) < 20$. The rest of the results are for the instantaneous frequency magnitude: $\| \nabla\phi \| < 0.046$ for (c) and (d), $0.046 < \| \nabla\phi \| < 0.08$ for (e) and (f), $0.08 < \| \nabla\phi \| < 0.15$ for (g) and (h).